

Energy transfer in noble-gas mixtures: Penning ionization in He/Xe[†]

R. Shuker, A. Szöke, E. Zamir, and Y. Binur

Departments of Physics and Chemistry, Tel Aviv University, Tel Aviv, Israel

(Received 19 August 1974)

Following recent reports on strong uv and ir laser transitions in noble-gas mixtures, we attempted to determine the dominant precursor reactions leading to laser action. In this paper we present experimental results of time-dependent spectroscopy of the various species existing in He/Xe mixtures excited by fast transverse electrical discharges. We also present some parametric measurements of the He/Xe laser in the ir region. A plasma model is suggested for explaining the time behavior of the helium and xenon emissions. According to this model, which is justified by the experimental results, ir laser action in the He/Xe mixture is excited mainly by energy transfer from metastable helium atoms and molecules by Penning ionization of xenon atoms.

I. INTRODUCTION

Some successful attempts to get high-power lasers using noble gases or noble-gas mixtures as active media were reported recently.¹⁻⁴ This type of laser is of special interest because of its capability to operate in the ultraviolet and vacuum-ultraviolet (VUV) wavelength region. Many processes take place in the rare-gas plasma, leading to excitation of levels participating in the lasing transitions. Some of the rate constants and cross sections of these processes are as yet unknown, even for pure one-component rare gases.^{5,6} The situation becomes more complicated for mixtures since the relative pressures strongly affect discharge parameters such as electron density and temperature. The electronic energy-transfer mechanism in noble-gas mixtures, studied recently in our laboratory,⁷ has focused our attention on the need for more spectroscopic data to resolve the relative importance of the various plasma processes.

The purpose of this work is to study the role of helium in He/Xe mixture discharges by means of spectroscopic measurements in the low- and medium-pressure range (10^{-3} –1-Torr Xe in 20–200-Torr He). In particular, we wanted to clarify whether the excitation of Xe in the mixture increases only as a consequence of the changed discharge parameters^{3,4} or whether there is an additional excitation of Xe by energy transfer from He.

Three types of measurements were carried out: (a) time-dependent measurements to monitor the rise and decay times of the various fluorescence lines; (b) relative intensity measurements of these lines; and (c) parametric studies of a transverse discharge He/Xe laser.

The experimental results indicate the important

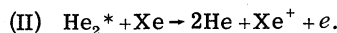
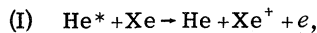
role of energy transfer from He* to Xe.⁸ In the pressure ranges mentioned above, the helium metastables ionize Xe atoms, which after recombination with free electrons cascade down to levels participating in the laser transitions. Although excitation and ionization of Xe by inelastic electron collisions occur during the short-current pulse, the main excitation of Xe and emission from Xe is due to Penning ionization of Xe atoms by helium metastables with a contribution by charge transfer.

In Sec. II, we suggest a model that explains the main processes occurring in pure and mixed gas discharges. In Sec. III, the experimental procedures and results are given. Finally, the model for the He/Xe mixture is discussed and justified according to experimental results.

II. PLASMA MODEL

The dynamic processes in the pure-gas discharges are extensively treated in the literature.⁹⁻¹³ Table I lists the most important processes in pure-helium discharges. Similar processes occur in pure-xenon discharges. However, the cross sections and rate constants are different. In particular the recombination of xenon is dissociative. In helium, inelastic collisions are most important processes during the current pulse, at the end of which, the electrons cool off very fast. Molecular species formation takes place during the early afterglow. Recombination also occurs and for a helium pressure of 20 Torr and a free-electron density of 10^{13} cm⁻³, the recombination time is 5×10^{-6} sec. The recombination, followed by fast radiative cascade of the higher excited levels, results in high metastables density. The metastables produce ions via efficient self-Penning-ionization mechanism.

When xenon is added to the helium to make a He/Xe mixture, the helium-metastable lifetime is reduced because of Penning ionization of the xenon atoms:



The cross section for Reaction I is¹⁴ $\sigma = 1.4 \times 10^{-15} \text{ cm}^2$ and that of Reaction II is of the same order of magnitude.¹⁰ Self-Penning-ionization of two xenon metastables also exists, but it is only important at a later period when the density of helium metastables drops. This process is assumed to have the same cross section as of Reactions I and II.

The xenon ions are produced both by Reactions I and II and directly by collisions with hot electrons in reactions similar to 2 and 3 of Table I. They later recombine with free electrons and then cascade down radiatively until reaching the xenon metastable level. The rate of change of the xenon-ion-density is given by

$$\frac{d[\text{Xe}^+]}{dt} = (\langle \sigma \nu \rangle_{\text{at}} [\text{He}^*] + \langle \sigma \nu \rangle_{\text{mol}} [\text{He}_2^*]) [\text{Xe}] - \alpha_{\text{Xe}} [\text{Xe}^+] [e], \quad (1)$$

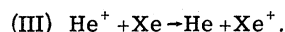
where α_{Xe} is the effective recombination coefficient for xenon ions and $[A]$ is the density of species A. For pure xenon in moderate pressures (1–100 Torr) the recombination coefficient for Xe_2^+ is known to be high¹⁵ ($1.4 \times 10^{-6} \text{ cm}^3 \text{ sec}^{-1}$). However, in the case of He/Xe mixtures when the xenon partial pressure is of the order of 10^{-3} Torr, and the density of electrons is determined by the density of helium ions rather than that of xenon ions, the rate of producing Xe_2^+ is as low as 8 sec^{-1} .¹⁶ Thus dissociative recombination is negligible in He/Xe mixture and the dominant

process is collisional-radiative recombination.¹⁷ The rate for this kind of recombination has not been measured, but one can estimate¹² that it is of the order of $10^{-9} \text{ cm}^3 \text{ sec}^{-1}$.

The time behavior of the XeI lines is proportional to the rate of change of the Xe^+ population because of the short radiative lifetimes of the xenon levels. Equation (1) shows that the rate of populating the xenon-ion ground state is determined by the helium-metastable lifetime, while its depopulation is determined by the rate of formation and the xenon-ion recombination rate. Since the last process is faster, the Penning ionization by He metastables dominates the time decay.

Within the framework of our model, the doubly ionized xenon is excited directly by collisions of singly ionized xenon with hot electrons during the current pulse. They are also being formed by collisions of molecular and atomic helium metastables with ground-state Xe^+ .

Charge transfer from He^+ to Xe is possible; this is described by the reaction



Measured cross sections for charge transfer are available only for helium ions with kinetic energy above 2 eV.¹⁸ This energy is quite high compared with that available in our experiments. Nevertheless, using the value for 2 eV which is 10^{-15} cm^2 with concentration of $3 \times 10^{14} \text{ cm}^{-3}$ of helium ions and xenon pressure of $\frac{1}{100}$ Torr, the characteristic time is about 30 μsec . However, spectroscopic measurements¹⁹ do not support such a high cross section and the characteristic time would be much longer under the conditions of our experiments. Charge transfer via a more complicated process can exist whereby a $[\text{HeXe}]^+$ ion complex

TABLE I. Plasma processes in pure-helium discharges.

Process	Comments
1. $\text{He} + e \rightarrow \text{He}^* + e$ } 2. $\text{He} + e \rightarrow \text{He}^+ + e$ } 3. $\text{He}^* + e \rightarrow \text{He}^+ + e$ }	{ Inelastic electron-atom collisions. Fast processes important during the current pulse; process 3 exists during the afterglow period too.
4. $\text{He}^+ + 2\text{He} \rightarrow \text{He}_2^+ + \text{He}$ } 5. $\text{He}^* + 2\text{He} \rightarrow \text{He}_2^* + \text{He}$ }	{ Molecular species formation, quadratic pressure dependence.
6. $\text{He}^+ + e \rightarrow \text{He} + h\nu$	Radiative recombination.
7. $\text{He}_2^+ + e \rightarrow \text{He}^* + \text{He}$	Dissociative recombination.
8. $\text{He}^+ + e + e \rightarrow \text{He}^* + e$ } 9. $\text{He}_2^+ + e + \text{He} \rightarrow \text{He}_2^* + \text{He}$ }	{ Collisional radiative recombination: The coefficient is (Ref. 5) $\alpha_{\text{He}} = (1.3 + 0.041p) \times 10^{-8} \text{ cm}^3 \text{ sec}^{-1}$ where p is the pressure in Torr.
10. $\text{He}^* + \text{He}^* \rightarrow \text{He}^+ + \text{He} + e$ } 11. $\text{He}_2^* + \text{He}_2^* \rightarrow \text{He}_2^+ + e + 2\text{He}$ } 12. $\text{He}_2^* + \text{He}^* \rightarrow \text{He}^+ + e + 2\text{He}$ }	{ Self-Penning-ionization important during the afterglow. The cross section is (Ref. 13) 10^{-14} cm^2 .

is formed, decays, and then dissociates into a Xe^+ and a helium ground state. This process is of minor importance in our experiments. Oskam²⁰ measured conversion coefficients for the production of heterogeneous ions of He^+ with Ne, Ar, and Kr. He concluded that the probability for such process decreases with the increase in difference between ionization potentials of He and the other atom. Even if we are using the conversion coefficient for $[\text{HeKr}]^+$ formation, which is $40 \text{ sec}^{-1} \text{ Torr}^{-2}$, the characteristic time for the formation of $[\text{HeXe}]^+$ is long compared with other processes in our experiment. Our model for the plasma processes in He/Xe discharges is shown in Fig. 1.

III. EXPERIMENTAL PROCEDURES AND RESULTS

The experimental setup consists of a discharge tube that is coupled via a LiF window to a McPhearson model 218 evacuable monochromator equipped with an EMI 9524S photomultiplier. Two different designs of discharge tube were used: an improved Tanaka-type lamp²¹ equipped with coaxial return leads, and a transverse discharge tube with two rod electrodes 10 cm long and 2.5 cm apart. Details of the latter are discussed elsewhere.²²

A schematic diagram of the discharge electrical circuit is given in Fig. 2. Special care was taken to reduce the self-inductance of this circuit, and pulses as short as 40-nsec width at half-peak were obtained. A typical current pulse is shown in Fig. 3. Parametric studies of the laser behavior were performed in a 60-cm-long transverse discharge tube that is excited by a circuit similar to that

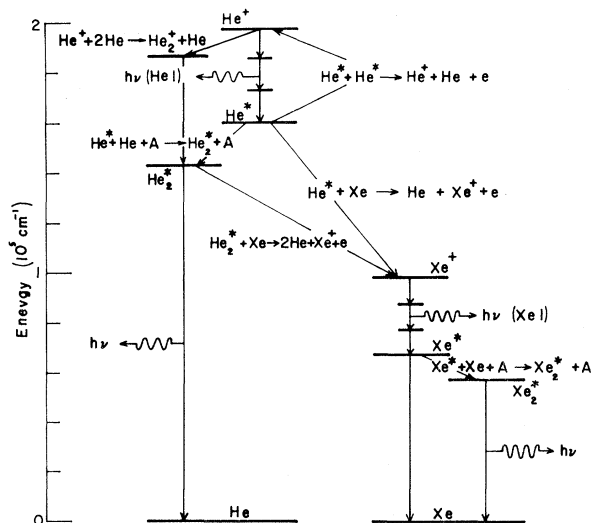
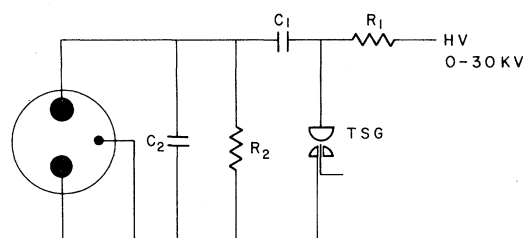


FIG. 1. Schematic representation of the plasma model. The most important processes taking place in a He/Xe mixture are indicated.



$C_1 - 0.01 \mu\text{F}$	$R_1 - 10 \text{ M}\Omega$
$C_2 - 4 \times 0.002 \mu\text{F}$	$R_2 - 2 \text{ M}\Omega$
TSG - E G & G	GP - 14 B

FIG. 2. Electrical network of the discharge circuit. For transverse-discharge spectroscopy tube $c_1 = 500 \text{ pF}$, $c_2 = 1000 \text{ pF}$, $R_1 = 2 \text{ M}\Omega$, $R_2 = 1 \text{ M}\Omega$, for triggering unit (TSG) a fast-hydrogen tyatron was used. For the laser tube, $C_1 = C_2 = 0.02 \mu\text{F}$, $R_1 = 10 \text{ M}\Omega$, $R_2 = 1 \text{ M}\Omega$ and for triggering unit (TSG) a triggered spark-gap was used.

shown in Fig. 2 except for the main capacitor C_1 and the auxiliary capacitor C_2 that were of $0.02 \mu\text{F}$ each. The rise time of the resulting discharge was fast enough to cause superradiant laser action in N_2 at 3371 \AA . The current pulse width varied around 100 nsec depending on gas pressure and mixtures. The laser tube had CaF_2 Brewster-angle windows and gold-coated mirrors of quite low quality. Laser power was coupled out through a 2-mm-diam hole in one of the mirrors. Laser output was measured with a Ge: Au detector through a Bausch & Lomb 500-mm monochromator.

All the spectral lines observed in pure helium and He/Xe discharges contain two components, a sharp one which follows the current pulse, and a delayed component to which we will refer as the afterglow. The laser output follows the same pattern²³ (Fig. 4). The sharp component results from inelastic electron collisions. Direct-excitation probabilities are approximately directly proportional to electrical-dipole transition probabilities and indeed the observed sharp component of the optically allowed $^1P_1 \rightarrow ^1S_0$ transition of Xe I

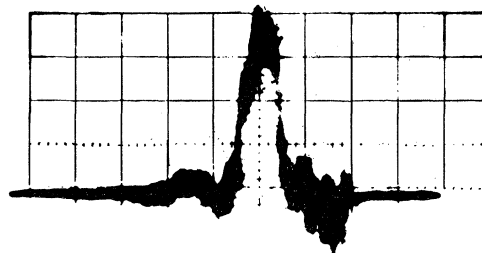


FIG. 3. Current pulse in the transverse-discharge spectroscopic tube, filled with 0.5-Torr xenon and 35-Torr helium. Time scale is 50 nsec/division.

was relatively stronger than the forbidden $^3P_1 - ^1S_0$ transition. The afterglow component is of more interest because most of the laser energy is emitted in this period of time.

In pure helium, only He I lines could be seen. However, the existence of ground-state ionized helium (He^+) is of course essential for the discharge. The afterglow component of the He I lines has a fast risetime, less than 200 nsec and a slow decay time which is pressure dependent. This decay time decreases from 30 μsec for pressure of 10 Torr to 1.5 μsec for 60 Torr. It changes approximately as p^{-2} . One should note that the He I decay times are not diffusion limited. In our transverse discharge tube with a diameter of 2 cm, the diffusion time of 20–100 Torr is much longer²⁴ than the times measured in our experiment.

In He/Xe mixtures one can find Xe I and Xe II lines as well as few Xe III lines. The intensity of the spectral lines varied with xenon concentration. At 1-Torr xenon in 50-Torr helium there is almost no helium emission. The helium lines become stronger as the xenon partial pressure is lowered. At xenon partial pressure of 10^{-3} Torr in 50-Torr helium, the helium lines reach the same intensity as in pure helium. With these concentrations the lines of Xe I, and Xe II appear very strongly, showing that the number of excited xenon atoms grows rapidly as the Xe concentration is lowered. In fact, at 10^{-3} -Torr Xe in 50-Torr He the fractional excitation (per xenon atom) of Xe I is about 15 000 times higher than in pure Xe.

The time dependence of the Xe I lines in a He/Xe mixture differs from that of the Xe II lines. Xe II lines have, like He I lines, a fast rise time of less than 200 nsec. Xe I lines have a much longer rise time which seems to follow the decay time of He I lines. However, the signal-to-noise ratio of our system is such that we cannot be positively sure whether these two times are identical. The decay time of Xe I lines is always longer than the decay of He I lines. It changes from 32 μsec at 2.5×10^{-3} -Torr Xe in 20-Torr He to 4 μsec at 1-Torr Xe in 20-Torr helium. The decay time of Xe II lines for high (1-Torr) xenon partial pressure is shorter than the He I decay time while for low (2.5×10^{-3} Torr) xenon partial pressure this time is longer. This dependency is discussed elsewhere.²⁵ The rise and decay times of some representative helium and xenon lines are summarized in Table II. Typical oscillograms are shown in Fig. 5.

Because of equipment limitations of the laser experiment, only the strongest Xe lines (namely the 1.732-, 2.026-, 2.651-, 3.508-, and 3.652- μm lines) could be observed. It should be pointed out that the output intensity changes very little

when the Xe partial pressure changes between 0.2 and 6 Torr. The dependence on He pressure is almost linear between 50 and 400 Torr.

A typical output pulse of the He-Xe laser at 2.026 μm is shown in Fig. 4. This picture was taken in a mixture of 2-Torr Xe and 50-Torr He. It has a sharp component which appears simultaneously with the current pulse and a delayed component which carries most of the energy with a peak 4–8 μsec after the current pulse. All the laser lines show the delayed component, the sharp one is most pronounced in the 2.026- μm line.

IV. DISCUSSION

There are three possible channels of excitation mechanism for the xenon atoms in the He/Xe mixture: (a) a one-step direct-excitation mechanism, which is compatible with the observation that the upper levels of xenon-laser lines in general have opposite parity to that of the ground-state level of the xenon atom²⁶; (b) a one-step direct ionization of the xenon atoms and consequent recombination of xenon ions with a free electron to produce excited xenon atoms; (c) energy transfer from helium molecules, atoms or ions to form xenon ions.

Direct electron collisions can cause significant excitation only during the current pulse when electrons have sufficient energy. This excitation channel can only explain the sharp pulse of the fluorescence and of the laser emissions. The fact that the presence of helium is essential for laser action in He/Xe mixture and the enhancement of the xenon lines in the afterglow fluorescence was explained^{3,4,27} by the assumption that the role of helium is to lower the electron mobility and consequently to give rise to higher fields. It also makes available a larger number of electrons at higher energy than would be obtained in a pure-xenon discharge. However, the electron tempera-

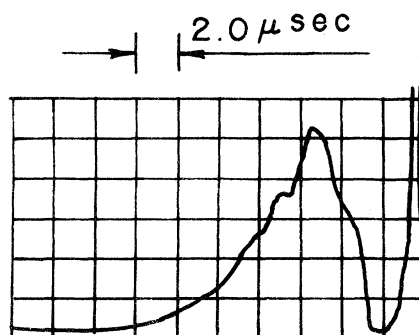


FIG. 4. Typical output pulse of the He/Xe laser at 2.026 μm . The mixture is 2-Torr xenon and 50-Torr helium.

TABLE II. Typical rise and decay times (in microseconds) of He I, Xe I, and Xe II lines experimentally measured.

		1 Torr Xe, 20 Torr He	5×10^{-2} Torr Xe, 20 Torr He	2.5×10^{-3} Torr Xe, 20 Torr He
Xe I (4671 Å)	Rise time	0.25	7	10
	Decay time	4	25	32
Xe II (4462 Å)	Decay time	0.75	5	12
He I (4471 Å)	Decay time	2	7	10

ture in He/Xe is most probably less than the electron temperature in a pure-helium discharge, which is about twice the electron temperature in a pure-xenon discharge.²⁸ The different value of T is a result of the fact that the ionization energy of helium is about twice that of xenon. The probability of ionization of xenon atoms by collision with electrons is given by

$$n_e \int_{E_I}^{\infty} f(E) \sigma(E) v(E) dE,$$

where n_e is the electron density, $\sigma(E)$ is the cross section for direct excitation and ionization of xenon atoms, $v(E)$ is the electron velocity, $f(E)$ is the distribution function, T_e is the electron temperature, and E_I is the ionization energy of xenon. $\sigma(E)$ may be taken as a constant for the energy ranges where $E \approx kT_e$. Taking into account the fact that the electron density does not change significantly in the various mixtures as reflected by the current measurements, we found that increase in electron temperature in He/Xe relative to that in a pure-xenon discharge can account for an intensity enhancement of 300 at the most as opposed to the factor of 15 000 which was obtained experimentally. Not only can the enhancement of Xe I fluorescence not be fully explained by the higher electron temperature in the mixture discharge but also its persistence in the afterglow period when the current pulse ends and the electron temperature decreases very fast. One must therefore conclude that enhancement of fluorescence and the consequent laser action in He/Xe mixture is for a large part due to energy transfer from helium. This may be done either by Penning ionization of xenon by helium metastables, or charge transfer from helium ions to xenon atoms. The experimental results show that in the mixtures there is no special enhancement of the fluorescence from xenon-ion levels in which charge transfer from helium ions might end. Thus, assuming that charge transfer is possible only from the xenon ground state, this process plays a minor role in the excitation of xenon atoms and only in

the very late period of the afterglow where the emission is negligible. The more complicated process of producing the $[\text{HeXe}]^+$ complex is under investigation and seems to be of minor importance too.

We therefore conclude that the dominant excitation mechanism of the xenon atoms is via Penning ionization by atomic and molecular helium metastables. According to this model, the rise time of the Xe I line should be equal to the decay time of the He I line and will be determined by Penning-ionization rates. The decay time of the Xe I line seems to be determined by the recombination time of xenon ions with free electrons, and the long tail is due to the self-Penning-ionization of the xenon metastables. The sequence of processes taking place in the discharge as concluded from the experimental evidence is as follows: During the current pulse a direct excitation and ionization of both helium and xenon atoms occur. This is followed by creation of He_2^+ and He_2^* and by recombination of He^+ and He_2^+ to excited levels which cascade down radiatively to the corresponding metastable levels. The last ones cause Penning ionization of both helium and xenon atoms. The decay time of the He I fluorescence is determined by the lifetime of the helium metastable. Increasing the partial pressure of xenon in the mixture decreases the He I decay time. The Xe I time behavior exhibits a rise time similar to the decay time of He I lines which is compatible with the assumption of the Penning ionization of xenon. The decay time of Xe I is determined by the recombina-

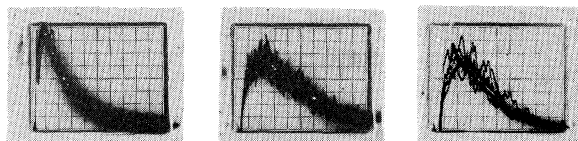


FIG. 5. Oscilloscope traces of few typical fluorescence lines in He/Xe mixtures of 2.5×10^{-3} -Torr xenon in 20-Torr helium: (a) He I line (4471 Å); time scale is 5 $\mu\text{sec}/$ division. (b) Xe I line (4671 Å); time scale is 10 $\mu\text{sec}/$ division. (c) Xe II line (4462 Å); time scale is 5 $\mu\text{sec}/$ division.

tion time of xenon ions, and has a long tail due to the slow loss of xenon metastables by the self-Penning effect. Helium metastables play the main role in the ionization and thereby the excitation

of xenon and in the lasing action of He/Xe mixtures. Energy transfer via Penning ionization is the main cause for enhancement of xenon excitation and emission.

†This work is supported by U. S. Air Force under Grant No. AFOSR-73-2518.

¹H. A. Koehler, L. J. Ferderber, D. L. Redhead, and P. J. Ebert, *Appl. Phys. Lett.* **21**, 198 (1972).

²P. W. Hoff, J. C. Swingle, and C. K. Rhodes, Livermore Preprint UCRL 71715, April 1973 (unpublished).

³S. E. Schwarz, T. A. De Temple, and R. Targ, *Appl. Phys. Lett.* **17**, 305 (1970).

⁴R. Targ and M. W. Sasnett, *IEEE J. Quantum Electron.* **QE-8**, 166 (1972).

⁵A. Wayne Johnson and J. B. Gerardo, *Phys. Rev. A* **5**, 1410 (1971).

⁶J. Stevefelt and F. Robben, *Phys. Rev. A* **5**, 1502 (1972).

⁷A. Gedanken, J. Jortner, B. Raz, and A. Szöke, *J. Chem. Phys.* **57**, 3456 (1972).

⁸Discussed by the authors in the VII International Quantum Electronic Conference, Montreal, Canada, May 1972 (unpublished).

⁹W. B. Peatman and J. P. Barach, *J. Chem. Phys.* **58**, 2638 (1973).

¹⁰D. M. Bartell, G. S. Hurst, and E. B. Wagner, *Phys. Rev. A* **7**, 1068 (1973).

¹¹A. Wayne Johnson and J. B. Gerardo, *Phys. Rev. Lett.* **28**, 1096 (1972).

¹²J. N. Bardsley and M. A. Biondi, in *Advances in Atomic and Molecular Physics*, edited by D. R. Bates (Academic, New York, 1970).

¹³A. V. Phelps and J. P. Molnar, *Phys. Rev.* **89**, 1202 (1953).

¹⁴E. E. Benton and W. W. Robertson, *Bull. Am. Phys. Soc.* **7**, 114 (1962).

¹⁵H. J. Oskam and V. R. Mittelstadt, *Phys. Rev.* **132**, 1445 (1963).

¹⁶E. V. George and C. K. Rhodes, Lawrence Livermore Laboratory preprint UCRL-74 516, Jan. 73 (unpublished).

¹⁷V. F. Moskalenko, E. P. Ostapchenko, and V. A. Cherinkov, *Opt. Spektrosk. (Acad. Nauk SSSR Otd. Fiz.-Mat. Nauk)* **33**, 308 (1972) [*Opt. Spectrosc.* **33**, 163 (1972)].

¹⁸W. B. Maier II, *Phys. Rev. A* **5**, 1256 (1972).

¹⁹M. Lipeles, R. Novick, and N. Tolk, *Phys. Rev. Lett.* **15**, 815 (1965).

²⁰M. J. Oskam, *Philips Res. Rep.* **13**, 401 (1958).

²¹B. Raz, J. Magen, and J. Jortner, *Vacuum* **19**, 571 (1969).

²²Y. Binur, R. Shuker, and A. Szöke, *Rev. Sci. Instrum.* (to be published).

²³V. D. Dandawate, G. C. Thomas, and A. Zembrod, *IEEE J. Quantum Electron.* **QE-8**, 918 (1972).

²⁴R. A. Gerber, G. F. Sauter, and H. S. Oskam, *Physica* **32**, 2173 (1965).

²⁵R. Shuker, Y. Binur, and A. Szöke (unpublished).

²⁶O. Andrade, M. Gallardo, and K. Bockasten, *Appl. Phys. Lett.* **11**, 99 (1967).

²⁷A. B. Dager and O. M. Stafssudd, *Appl. Opt.* **10**, 2690 (1971).

²⁸A similar argument was given for He/Ar mixture by C. S. Willet, *Appl. Opt.* **11**, 1429 (1972).

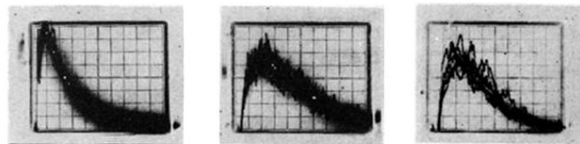


FIG. 5. Oscilloscope traces of few typical fluorescence lines in He/Xe mixtures of 2.5×10^{-3} -Torr xenon in 20-Torr helium: (a) He I line (4471 Å); time scale is 5 μsec /division. (b) Xe I line (4671 Å); time scale is 10 μsec /division. (c) Xe II line (4462 Å); time scale is 5 μsec /division.